HIGH RESOLUTION OPTICAL TIME DOMAIN REFLECTOMETRY AND ITS APPLICATIONS

by

Bernd D. Zimmermann

Thesis submitted to the Faculty of the

Virginia Polytechnic Institute and State University

in partial fulfillment of the requirements for the degree of

MASTER OF SCIENCE

in

ELECTRICAL ENGINEERING

APPROVED:

Dr. R. O. Claus

Dr. R. J. Pieper

Dr. C. W. Bostian

January, 1988
Blacksburg, Virginia

HIGH RESOLUTION OPTICAL TIME DOMAIN REFLECTOMETRY AND ITS APPLICATIONS

by

Bernd D. Zimmermann

(ABSTRACT)

High resolution Optical Time Domain Reflectometry (OTDR) measurements have recently allowed spatial resolutions of less than one millimeter. These capabilities indicate that OTDR techniques may be suitable for non-conventional applications such as the determination of fiber strain. This thesis presents an investigation of how high resolution OTDR techniques can be used in such applications. The concept of fiber segmentation via partially reflective optical splices for local strain measurements is discussed both from a theoretical and practical standpoint. Experimental results demonstrating the feasibility of such local strain measurements are also given. Another part of this investigation considers the practical details of the proposed strain measurement technique, addressing such topics as launching conditions, and environmental factors. Possible applications of the local strain measurement techniques, such as two- and three-dimensional stress analysis, and strain determination of fiber optic cables, are also presented. These applications also include the development of small, easy to manufacture elastomeric optical splices, which were shown to

yield acceptable performance (< 0.2 dB losses) for multimode fibers.

ACKNOWLEDGMENTS

I would like to express my sincere appreciation to for always offering his patience and dedication during many experiments. Without his knowledge and experience much of the related work would have been difficult if not impossible to implement.

Many thanks also go to my advisor, Dr. R. O. Claus, who has always been encouraging and helpful during my thesis research, and to Dr. J. P. Marton of Opto-Electronics for many helpful discussions.

Last, but not least, I would like to thank all of the fellow graduate students and assistants at the Fiber and Electro-Optics Research Center, who have made my stay at Virginia Tech so enjoyable.

TABLE OF CONTENTS

LIST OF TABLES

LIST OF FIGURES

Chapter I

INTRODUCTION

Optical Time Domain Reflectometry (OTDR) is one of the tools with which optical fibers can be characterized. OTDR techniques allow the determination of fiber length and attenuation, and can locate fiber faults, splices, and other reflective imperfections. Splice and connector losses can also be determined using these techniques.

The basic OTDR measurement system consists of a pulsed laser diode, a beamsplitter, a detector, a pulse delay generator, and an oscilloscope. The laser diode launches optical pulses into the optical fiber to be characterized, which scatters a portion of the forward traveling light energy back towards the beamsplitter and detector. The output of the detector is sampled and displayed on the CRT of an oscilloscope. A block diagram of such a system is shown in Figure 1.1. More detailed information on the operation of the basic OTDR system can be found in [1].

A typical OTDR system as the one depicted in Figure 1.1 usually uses high energy light pulses with pulse Full Width Half Maxima (FWHM) in the order of 5 ns or above [2-4]. This allows the detection of low amplitude, intrinsic Rayleigh

backscattered power on one hand, but yields poor distance resolution and large "dead zones" on the other.

To obtain a distance resolution in the sub-millimeter region, very narrow (< 35 ps FWHM) pulses must be used. These pulses, however, do not allow the detection of Rayleigh backscattered power due to their low energy content, unless photon counting techniques are used [5-7]. At the cost of not being able to measure fiber attenuation without photon counting, strain measurements on relatively short sections of fiber (1-5 m) become possible. This thesis investigates the feasibility of such high resolution OTDR measurements for the determination of fiber strain. Experiment results and particular applications, such as local strain measurements, will also be presented.

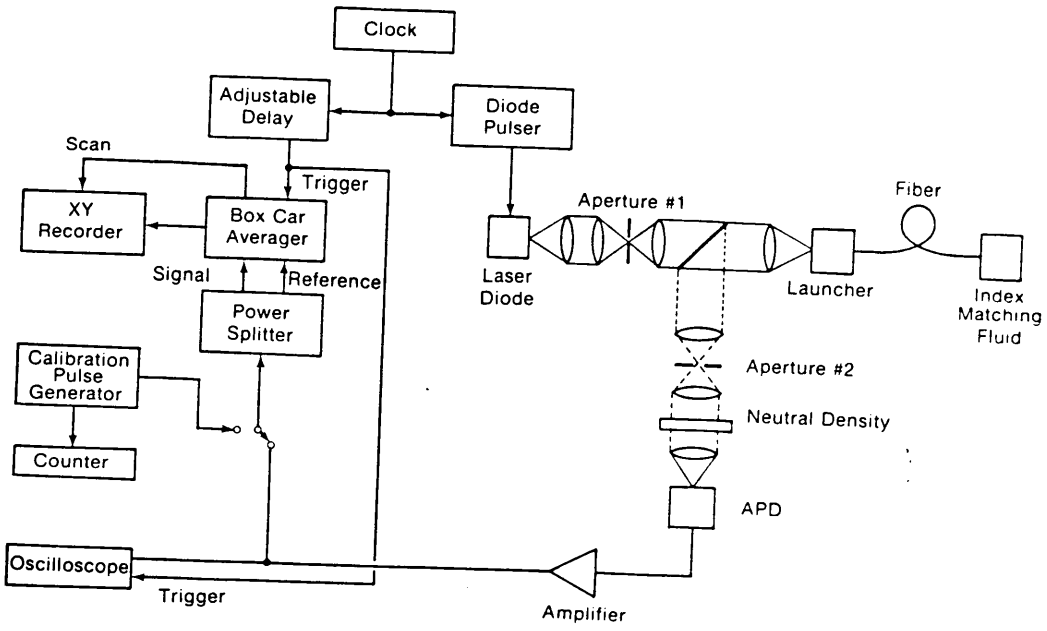

FIGURE 1.1 Block Diagram of the Basic OTDR System.

Chapter II

BACKGROUND

High resolution optical time domain reflectometry using sub-nanosecond pulsed lasers is considered a relatively new field in the fiber optics industry. A few companies such as Opto-Electronics and Laser Precision have recently started marketing high resolution OTDR systems [8]. Opto-Electronics, for example, offers a system which includes a low jitter (< 2 ps) pulse delay generator, a 35 ps FWHM pulsed laser, an APD detector, and a signal averager/processor. Their system allows sub-millimeter length measurements with a dynamic range of up to 44 dB. Applications of Opto-Electronic's unit include absolute and relative distance measurements, locating connectors, couplers, reflective splices, breaks, or other reflective faults in fibers, monitoring Local Area Networks (LAN's), measuring connector performance, precise strain, and pulse delay changes, and determining strain and temperature coefficients of fiber group indices. Table 2.1 summarizes the characteristics of Opto-Electronics PFOS/SE10 OTDR system.

Other companies such as Siecor Corporation are using similar equipment to measure fiber strain in optical fiber cables during pull testing. Here, longer lengths (150 m) of fiber are being tested, which does not necessitate

sub-millimeter distance resolution [9]. In fact, one way time delay (as opposed to two way OTDR) techniques usually yield acceptable precision.

More specific applications such as local strain measurements on optical fibers via partially reflective splices are believed to be novel. Patent searches indicate that work using segmentation of optical fibers through splicing has been performed in the past [10]; however time domain principles were not involved. Asawa et al. used partially reflective optical splices as markers along the fiber (see Figures 2.1 a-c). The determination of fiber strain, though, was achieved indirectly by monitoring the drop in backscattered light intensity in particular regions of the fiber, and time shifts of the backreflected pulses from the splices were not considered. Others such as Henning et al. [11] used a multiplexed optical sensing system to monitor local fiber strain. A heterodyne scheme was employed which produced a detectable electric beat frequency signal. The modulation of that signal would vary with changes in length of the optical fiber. Figures 2.2 a) and b) depict the system used in Henning's work.

TABLE 2.1 Specifications of the Opto-Electronics PFOS/SE10 High Resolution OTDR.

Transmitter Outputs:

	820-900 nm	1300 nm
Multimode	200 mW (23dBm)	50 mW (17 dBm)
Singlemode	100 mW (20 dBm)	25 mW (14 dBm)

Receiver Sensitivities (SNR = 1):

APD	-27 dBm	-17 dBm
Ampl. APD	-43 dBm	-33 dBm

Resolution:	SNR = 50	SNR = 20	SNR = 10	SNR = 5
APD	0.1 mm	0.2 mm	0.4 mm	1.0 mm
Ampl. APD	0.3 mm	0.5 mm	1.0 mm	2.5 mm

Environmental:

10 C to 40 C operating

-15 C to 60 C storage

Optical:

Connectors: Standard ST, custom biconic, FC, D4, SMA.

Fibers: Compatible with 50/125, 100/140, or SM 125 OD fibers.

Interfaces:

- Requires sampling oscilloscope.
- RS 232 data port.

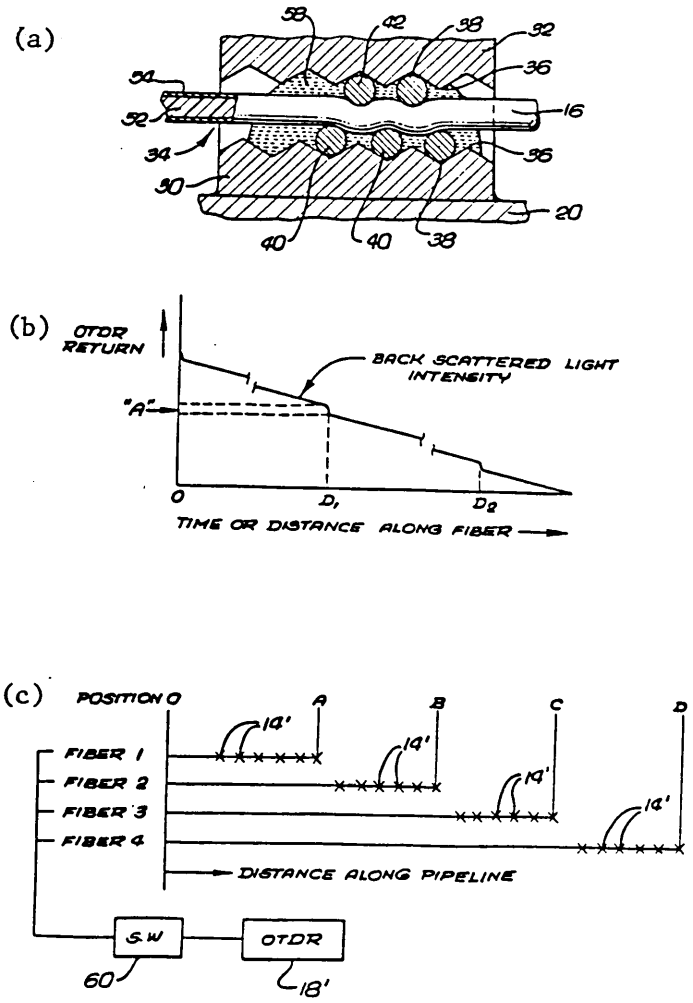

FIGURE 2.1 Microbend Transducer (a), OTDR Trace from Segmented Fiber (b), and Multiple Fiber Acsess Scheme (c), (Asawa et al.).

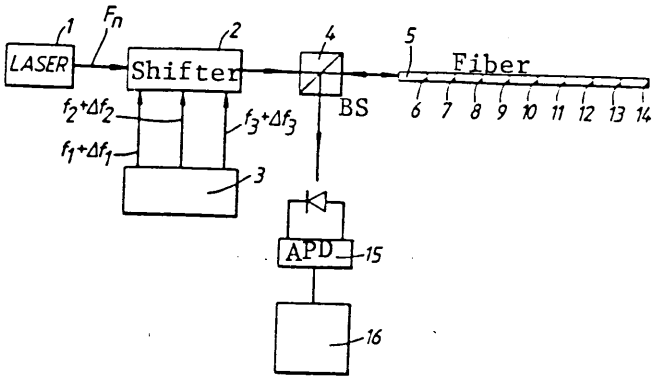

(a) Single Laser Multiplex Optical Sensing System

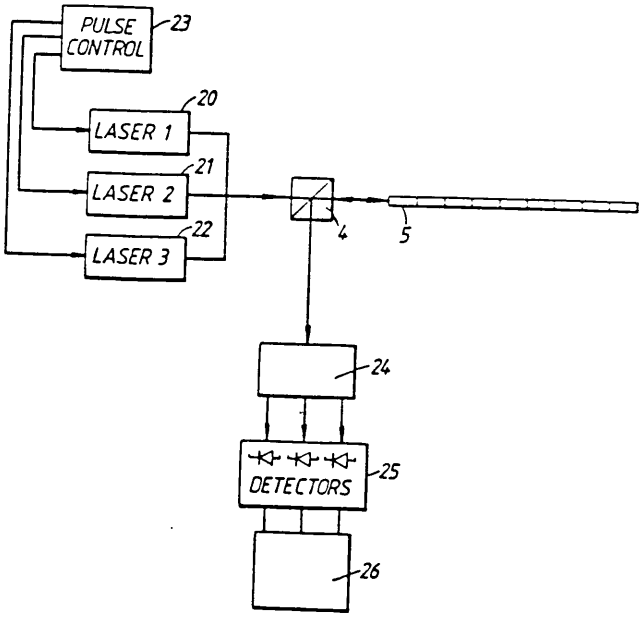

(b) Multiple Laser Multiplex Optical Sensing System

FIGURE 2.2 Heterodyne Schemes for Measuring Local Fiber Strain (Henning et al.).

Chapter III

THEORY

3.1 One Way Pulse Delay Measurements

The basic principles involved in fiber strain measurements using OTDR techniques can be related back to one way pulse delay measurement methods. Here, the length of the fiber, l_f, is given by:

$$l_f = \left(\frac{c}{n}\right)t \quad , \qquad (1)$$

where c is the speed of light, t is the time it takes the light pulse to travel down the fiber, and n is the group index of refraction of the fiber core. Differentiating equation (1) once, an expression for the amount of fiber elongation, dl_f, due to an applied strain, can be found as:

$$dl_f = \left(\frac{c}{n^2}\right)(ndt - tdn) \quad . \qquad (2)$$

The applied fiber strain, ε_f, is given by:

$$\varepsilon_f = \frac{dl_f}{l_f}$$

$$= \frac{dt}{t} - \frac{dn}{n} \quad . \qquad (3)$$

Equation (3) takes into consideration the changes of

group index with respect to the applied strain. The index vs strain relationship is linear, and "a" shall denote the slope of the line. "a" is a negative number that can be determined empirically or from theoretical models (see [12-14]). It is suggested, however, to find "a" empirically for a given fiber, since the models mentioned above assume single mode operation (i.e., all fiber modes propagate parallel to the fiber axis). A method to find "a" empirically is presented at a later point.

Assuming dn/n is given by:

$$\frac{dn}{n} = a\left(\varepsilon_f\right) \quad , \qquad (4)$$

equation (3) becomes:

$$\varepsilon_f = \left(\frac{\Delta t}{t}\right)\cdot\left(\frac{1}{1+a}\right) \quad , \qquad (5)$$

where Δt is the shift in pulse arrival time.

3.2 OTDR Measurements

Equation (5) is also valid for OTDR strain measurements, where the light pulse travels down the length of the fiber twice. In this case t denotes the time it takes the pulse to cover that length, and Δt is the time shift of the pulse resulting from fiber strain. Since for OTDR methods the pulse has to travel twice the distance than the pulse in one way

pulse delay methods, the strain resolution is improved by a factor of 2. This resolution, R_ε, is a function of the rise time, τ, of the probe pulse and the measurement SNR. The SNR of the measurement depends on the number of measurement averages and averaging time. As a rule of thumb, the SNR can be improved by a factor of the square root of the averaging time [2]. In typical OTDR systems the pulse FWHM, W_m, will limit the spatial resolution, R_s, to:

$$R_s = \left(\frac{W_m c}{2n}\right) \quad . \qquad (6)$$

3.3 Fiber Segmentation

In order to determine local fiber strain, the probing fiber needs to be segmented as shown in Figure 3.1. The method of segmentation is arbitrary from a theoretical standpoint; however, it will be seen that interfaces which yield Fresnel reflections are most advantageous. These reflections, separated in time by an amount proportional to the distance between segments, will be sent back towards the OTDR detector. This distance can vary among segments.

The distance, l_i, of the ith segment can be expressed in terms of the arrival times of its far and near end reflected pulses, t_i and t_{i-1}, as [15]:

$$l_i = \left(\frac{1}{2}\right)\left(\frac{c}{n}\right)(t_i - t_{i-1}) \quad . \qquad (7)$$

As strain is applied, l_i will change by an amount dl_i equal to:

$$dl_i = \left(\frac{c}{2}\right)\left(\frac{nd(t_i - t_{i-1}) - (t_i - t_{i-1})dn}{n^2}\right) \quad . \quad (8)$$

The strain, $\varepsilon_{f,i}$, in the ith segment can now be found, as in equation (3), to be:

$$\varepsilon_{f,i} = \frac{dl_i}{l_i}$$

$$= \frac{d(t_i - t_{i-1})}{(t_i - t_{i-1})} - \frac{dn}{n} \quad , \quad (9)$$

where dn/n is again taking into consideration the changes in index with respect to strain, and is given by:

$$\frac{dn}{n} = a\left(\varepsilon_{f,i}\right) \quad , \quad (10)$$

and "a" has been defined previously.

If equation (10) is substituted into equation (9),an expression for $\varepsilon_{f,i}$ can be obtained. Approximating the differentiating operator with a Δ notation, this yields:

$$\varepsilon_{f,i} = \left(\frac{\Delta t_i - \Delta t_{i-1}}{t_i - t_{i-1}}\right)\cdot\left(\frac{1}{1 + a}\right) \quad . \quad (11)$$

The expression given in equation (11) represents the basic principle which will allow the measurement of local strain. Δt_i and Δt_{i-1} will be measured as the segmented fiber is

subjected to strain. Knowing t_i, t_{i-1}, and "a" then allows the determination of the local strain, $\varepsilon_{f,i}$.

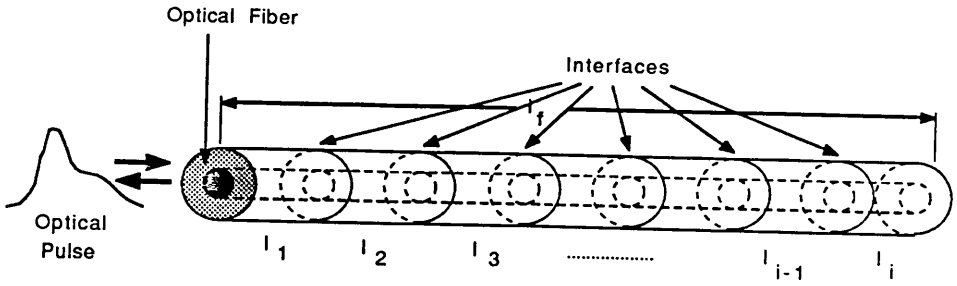

$$l_f = i \times l_i \qquad (l_1 = l_2 = \ldots = l_i)$$

FIGURE 3.1 Optical Fiber Segmented into Discrete Sections.

Chapter IV

THE SEGMENTATION DEVICE

4.1 The Partially Reflective Splice

Since the proposed local strain measurement technique was intended to be used for relatively short fibers, it was imperative that the segmentation device, which subsequently segments the probing optical fiber, would not entail any optical transient effects. It was therefore decided to choose partially reflective optical splices, which contained air gaps. These air gaps would yield Fresnel reflections at the segment interfaces.

Early splice prototypes consisted of Norland splice tubes mounted on brass strips. These devices, however, were too large for embedding purposes. The "air gap splice" had to measure less than 1.5 mm in diameter, and 2 cm in length to make structural strain measurements feasible. Therefore, a novel idea, which used the optical fiber coating itself as an alignment sleeve, was implemented. The aligned fibers inside the alignment sleeve were contained in a short (~ 1.9 cm) stainless steel tube (with an outer diameter of 1.2 mm) filled with epoxy (see Figure 4.1). The stainless steel tube and epoxy would serve as strain relief and maintain the air gap between fiber ends constant. This gap would vary in length

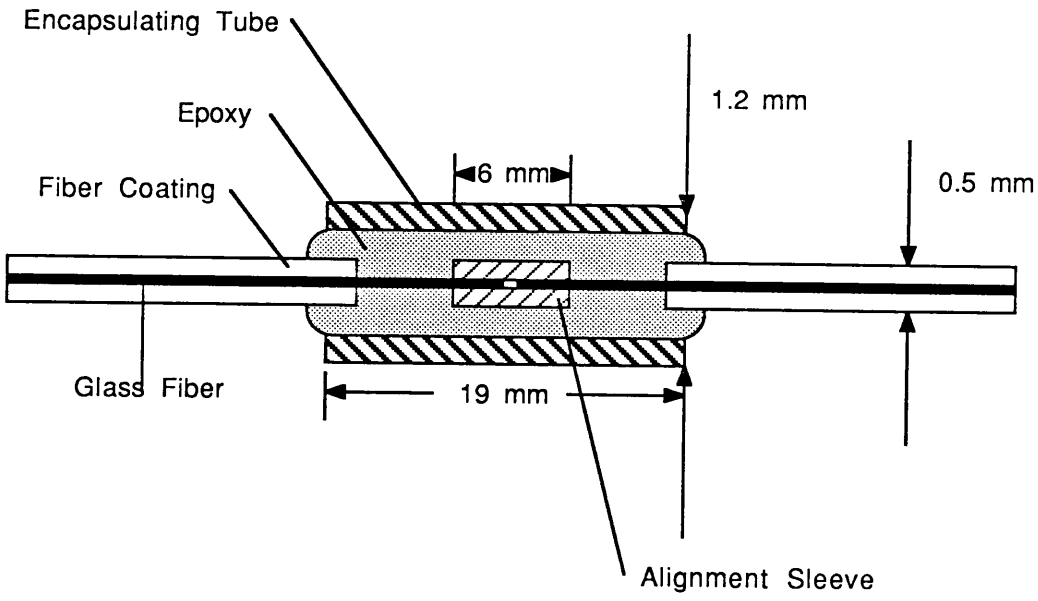

Note: Objects not Drawn to Scale

FIGURE 4.1 Partially Reflective "Air-Gap Splice".

between 5 and 50 micrometers.

4.2 The Splice Power Budget

It is obvious that only a finite number of splices can be connected in series before the backscattered pulses are too weak to be detected. A power budget for the "air gap splice" is given in [13]. This budget is based on the optical power losses involved with optical splices [16] and losses due to Fresnel reflections at the interfaces [17]. Assuming negligible lateral and angular misalignments, and considering only the longitudinal loss, L_{long}, and Fresnel loss, L_{Fres}, an average forward power loss per splice, L_{sp}, can be found:

$$L_{sp} \simeq L_{long} + L_{Fres} \quad \text{dB} . \qquad (12)$$

Where: $$L_{long} = 10 \log\left(\frac{r}{r + \bar{S} \tan(\sin^{-1}(NA))}\right)^2 \quad \text{dB} , \qquad (12a)$$

and: $$L_{Fres} = 10 \log(1-p)^2 \quad \text{dB}. \qquad (12b)$$

In equation (12b) "p" denotes the reflection coefficient between glass and the gap medium (which in this case is air) and is given by:

$$p = \left(\frac{n - 1}{n + 1}\right)^2 , \qquad (13)$$

where n denotes the average index of refraction of the fiber core. The quantities r, $\bar{S}$, and NA in equation (12) represent the fiber core radius, the average gap distance, and the fiber

numerical aperture, respectively.

For typical multimode fibers, the average forward splice loss for gaps on the order of 5-50 micrometers will range between 0.6 and 2.6 dB. The two-way power loss, L_{2way}, which allows the determination of the power reaching the detector for a fiber containing N splices, is:

$$L_{2way} = 2NL_{sp} + 10\log(p(1-p)) + L_f \quad \text{dB} . \quad (14)$$

L_f, the loss of the fiber, may be negligible for short lengths (< 10 m) of fiber. Furthermore, the two way loss may be reduced by up to 10 dB if a highly reflective mirror can be placed at the end of the fiber. This method, however, only applies for the far end pulse of the probing fiber; all other Fresnel back-reflected pulses will not be affected by the use of the mirror at the far end.

By solving equation (14) for N, and equating L_{2way} to the dynamic range of the OTDR system, it is possible to find the maximum number of in-line splices. For high dynamic range systems and low loss air gap splices, the maximum number of in-line splices may be as high as 50.

Chapter V

EXPERIMENTS

5.1 Determination of the Index-vs-Strain Coefficient

To determine the feasibility of the proposed fiber strain sensor, several experimental steps had to be performed. First, it was necessary to show that it is possible to measure the index-vs-strain coefficient, a. This was done using different types of few- and multi-moded fibers (85/125, 100/140, 9/125 um) and an operating wavelength of 904 nm.

The setup used is shown in Figure 5.1. It consists of a JJ Instruments load frame with a 1 KN load cell, a Photon Kinetics FOA-1000 OTDR, and a Tektronix 7854 oscilloscope with a 7S12 TDR plug-in. The pertinent characteristics of the OTDR and the oscilloscope are summarized in Table 5.1. Notice that the limiting factors of the experiment consist mainly of the 400 ps FWHM pulse from the FOA-1000 and the 50 ps jitter (unaveraged) of the 7S12 TDR.

The load frame would strain a given length of fiber up to a certain load, F. Knowing F, the crossectional area, A, of the glass fiber (ignore the strength contributions of the fiber coatings), and the Young's modulus, E, of silica glass ($E \simeq 70000\ N/mm^2$), fiber strain, ε_f, can be computed as:

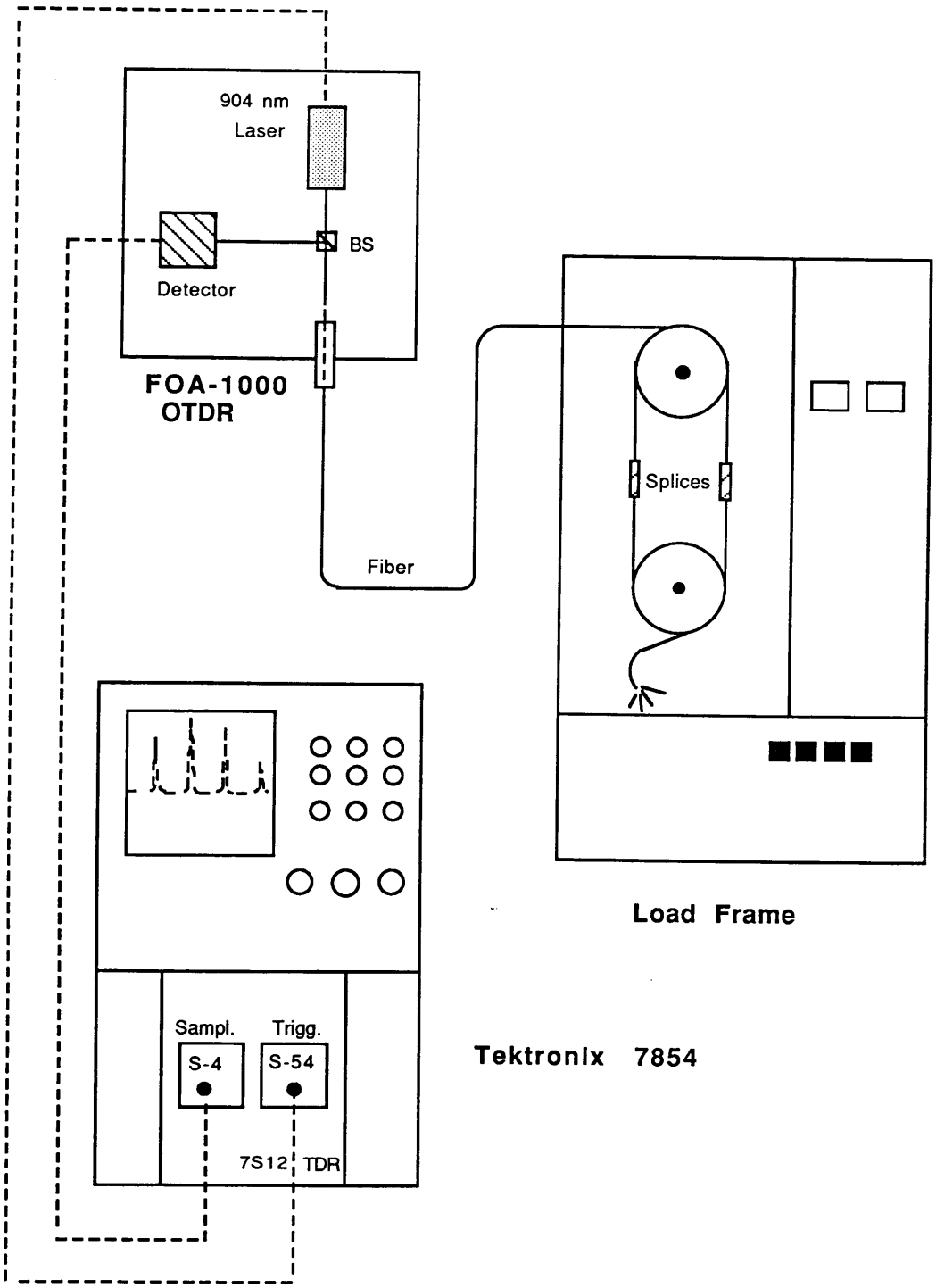

FIGURE 5.1 Experiment Set-Up for the Determination of the Index vs Strain Coefficient and the Measurement of Local Fiber Strain.

TABLE 5.1 Specifications of the Experiment System.

FOA 1000 OTDR:	
Laser	Pulsed GaAs @ 904 nm, 400 ps FWHM, <100 ps risetime.
Detector	Si APD, A = 700.
Sampling Scope:	
TDR	Tektronix 7S12 with S4 Sampling Head and S54 Pulse Generator, Includes 50 ps jitter Pulse Delay Generator.
JJ Lloyd Load Frame:	
Load Range	0 - 1000 N, 3 % accurracy.

$$\varepsilon_f \simeq \left(\frac{F}{A \cdot E}\right) \quad . \qquad (15)$$

Solving equation (5) for "a" yields:

$$a = \left(\frac{\Delta t}{t\varepsilon_f}\right) - 1 \quad . \qquad (16)$$

"a" was determined for the above mentioned fiber types using equation (16), where Δt was read off the CRT screen of the oscilloscope (see Figure 5.2). It is important to note that t here denotes only the time required for the pulse to travel through the length of fiber strung up in the load frame and excludes the time delays resulting from the fiber leading to and exiting the load frame "grippers".

For the larger core, multimode fibers the determination of "a" was done in the OTDR (2-way) mode, since only the alignment of the input end was required. For the 9/125 um (SM @ 1300 nm) few-moded fiber the Fresnel reflection from the far end of the fiber was too weak to be detected, so that "a" had to be measured using 1-way pulse delay techniques. This involved alignment of both the input and output ends of the fiber. Figure 5.3 shows a graph of $\Delta t/l_f$ vs ε_f for all three fiber types. Considering that "a" is proportional to the slope of these curves, it becomes evident that "a" varies among these three fiber types. The value of "a" ranged from -0.27 to -0.36.

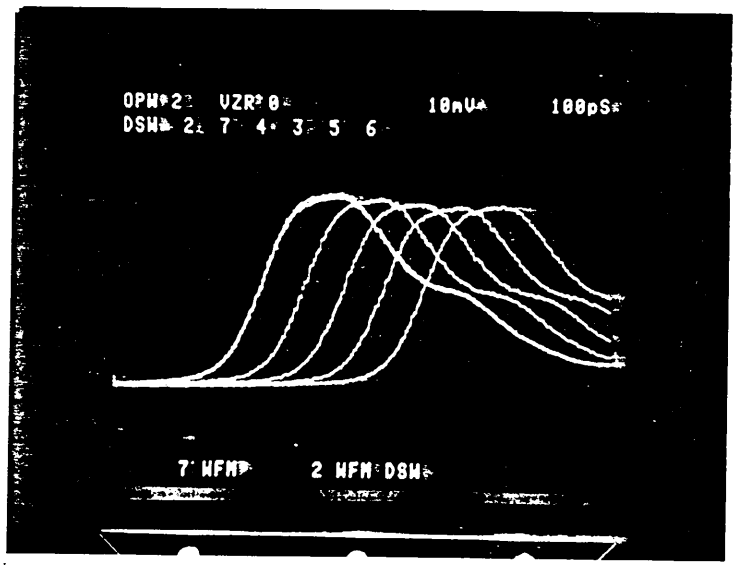

FIGURE 5.2 Far End Pulse Shift as Strain is Applied.

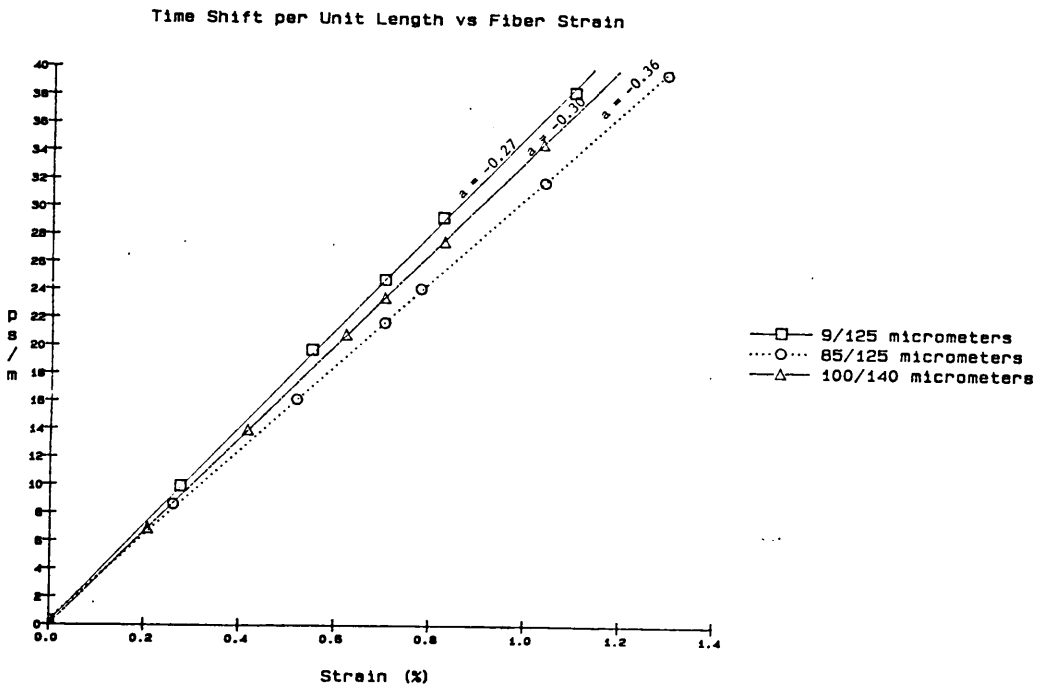

FIGURE 5.3 $\Delta t/l_f$ vs Applied Fiber Strain, ε_f for Three Different Fiber Types.

5.2 Implementation of the "Air Gap Splice"

The successful operation of the air gap splice depends on several crucial steps. First, it became obvious that the quality of fiber ends inside the alignment sleeve was one of the main contributors to low loss splices. Given the fact that low grade diamond cleavers were employed, it was difficult to achieve perfect, 90 degree ends. D. Marcuse studied the effects of imperfectly broken fiber ends in [17] and concluded that small deviations (~3.5 degrees) from the perfect 90 degree cleave could cause up to 50 % (3 dB) power losses.

Next, it was important to minimize the gap distance by applying compressive forces at both fiber ends during epoxy curing. Without the use of such forces, gaps as large as 75 micrometers were seen, even after the fibers had been butted up inside the alignment sleeve (see Figure 5.4). This was probably due to the elastic properties of the primary silicone coating of the alignment sleeve and the tight contact between fiber and coating.

Finally, it was imperative to avoid any foreign particles between fiber ends. This was very difficult to achieve, since insertion of the fiber ends into the alignment sleeve usually caused some scraping remains from the soft, primary coating. Nonetheless, given the above mentioned problems, it was still

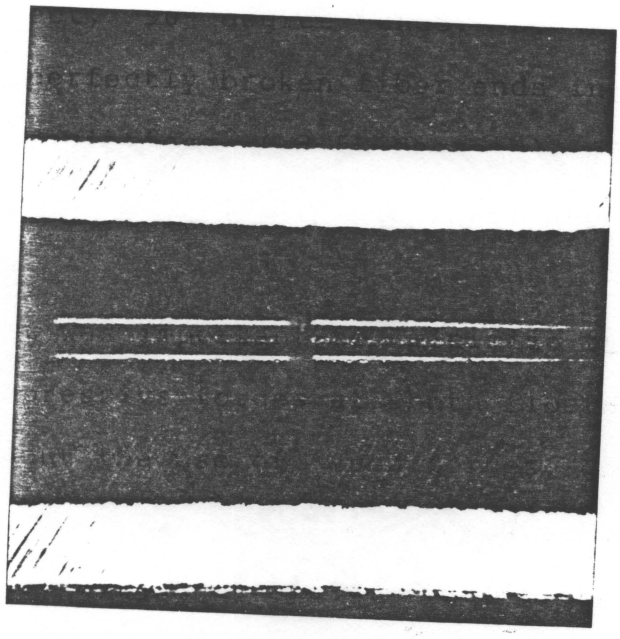

FIGURE 5.4 Photomicrograph of a Dissected Partially Reflective "Air Gap Splice".

possible to achieve air gap splices with losses as low as 0.4 dB, an indication that extremely small, uncontaminated air gaps were obtained. The average splice loss was ~ 0.8 dB.

5.3 Measuring Local Fiber Strain

Once "a" was determined, and acceptable air gap splices were being achieved, it became possible to measure local fiber strain. The same setup as shown before in Figure 5.1 was used. To avoid having to determine $t_i - t_{i-1}$ in equation (11) indirectly by measuring the length of fiber between the load frame grippers, it was decided to use a fiber containing two splices. This resulted in four back-reflected pulses on the CRT screen (see Figure 5.5). $t_2 - t_1$ was easily read off as the time separation between the second and third pulse, the first and fourth pulses indicating the arrival times of the reflections from the input and far ends of the fiber. A 100/140 micron fiber, whose "a" coefficient was measured to be -0.3, was used since it allowed maximum power propagation.

Assuming that the fiber strung up in the load frame was free to slide over the two frame mandrels, the strain in the middle section of the fiber should coincide with the overall strain in that fiber. The overall strain was determined by measuring the applied load, F and using equation (15). At 3.3 N the overall strain on the 100/140 micron fiber should be approximately 0.31 %. The strain, $\varepsilon_{f,2}$, in the middle section

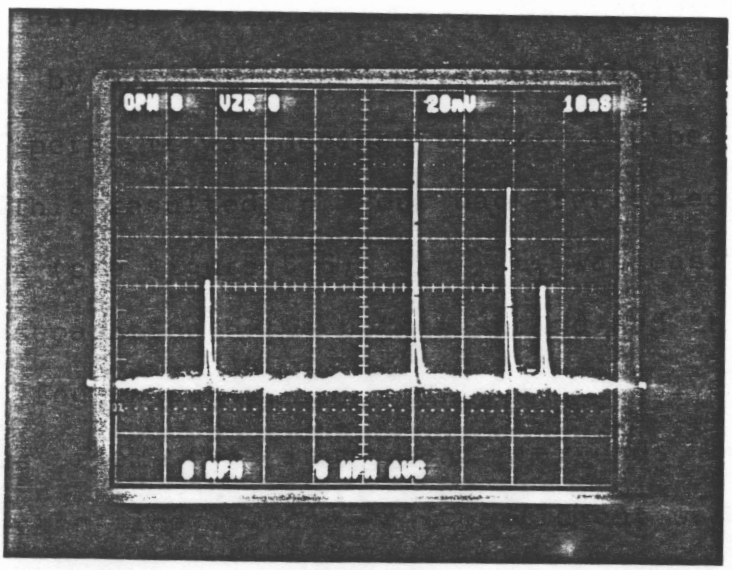

FIGURE 5.5 CRT Display of the Back Reflections of a Fiber Containing two "Air-Gap Splices".

of the fiber was determined using equation (11) with:

$t_0 = 0.0$ sec

$t_1 = 42 \times 10^{-9}$ sec

$t_2 = 61 \times 10^{-9}$ sec

$t_3 = 68 \times 10^{-9}$ sec

$\Delta t_1 = 73 \times 10^{-12}$ sec

$\Delta t_2 = 110 \times 10\text{-}12$ sec

$a = -0.30$

$\varepsilon_{f,2}$ turns out to be 0.28 %, close to the expected 0.31 % predicted above. The difference may be the result of ignoring the strength contribution of the fiber coatings, among others. Figure 5.6 shows the shift in time of the third pulse for 1.1 N load increments.

5.4 Multiple Splices

Although the optimum equipment and system for high resolution OTDR measurements were not available at the time of these experiments, it was still important to demonstrate the multi-splice capabilities of the proposed local strain sensor. With some patience it was possible to achieve a medium quality sensor containing five splices. The oscilloscope trace for such a sensor, with a mirror placed at the far end of the fiber to achieve a distinguishable far end reflection, is shown in Figure 5.7. Notice the "ghost" reflection to the right of the far end reflection. This ghost reflection is due

to the high power levels being launched back into the fiber from the mirror at the far end.

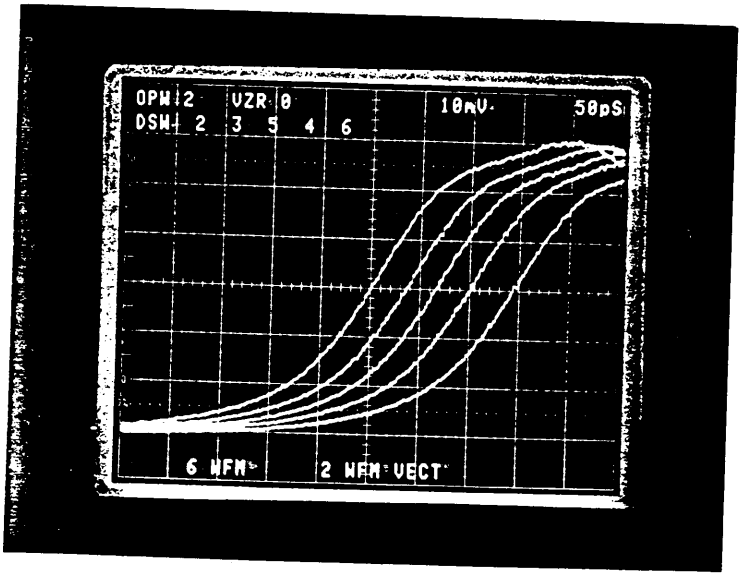

FIGURE 5.6 CRT Display of Δt_2 as the Applied Load is Increased in 1.1 ^{2}N Intervals.

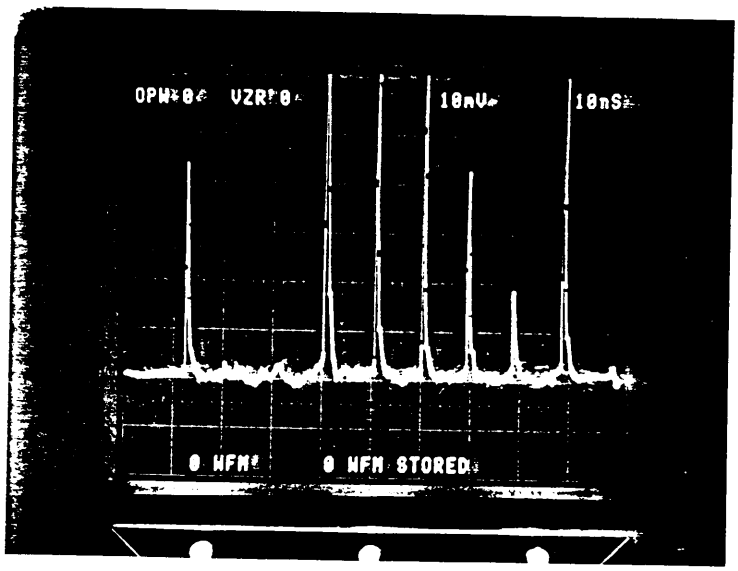

FIGURE 5.7 CRT Display of the Back Reflections of a Fiber Containing Five Splices with a Mirror Placed at the Far End.

Chapter VI

PRACTICAL CONSIDERATIONS

6.1 Launching Conditions

To obtain repeatable measurements with the proposed OTDR technique, it is important to consider certain factors which may affect the strain readings. First, it was observed that with certain fiber types (namely, 50/125 micron, step index fiber) it was crucial to use repeatable launching conditions. It was shown, that the shape of the back-reflected pulse(s) could vary with the way the fiber was being excited at the input stage. By selectively launching power into higher order modes the reflected pulse(s) seemed to arrive later in time (see Figure 6.1). This could very well mean, that the measurement may be susceptible to mode mixing due to applied stresses. This effect, of course, is not as noticeable with low dispersion, high bandwidth fibers such as graded index multimode or step index single mode fibers. If dynamic range does not limit the high resolution OTDR measurement it is therefore recommended to use single mode type fibers with dispersions of less than a few picoseconds per kilometer.

6.2 Temperature Effects

To be able to obtain sub-millimeter resolution measurements it is critical to consider any environmental

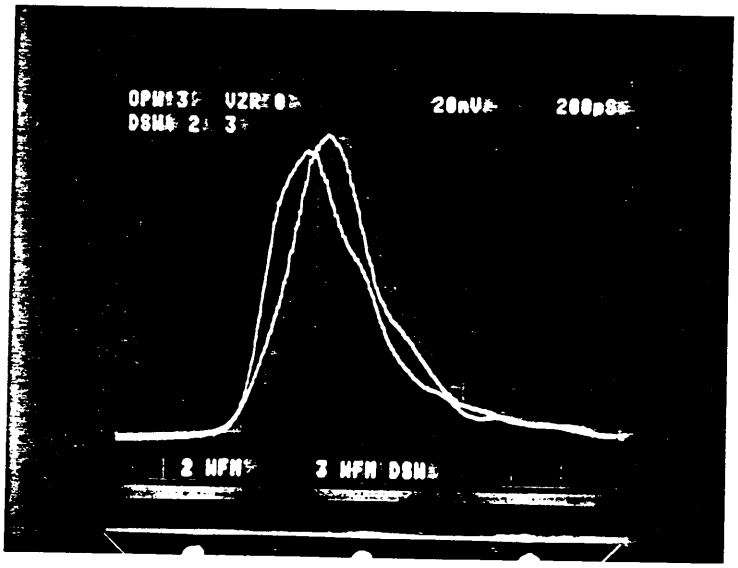

FIGURE 6.1 CRT Display Showing the Effect of Varying Launch Conditions on Pulse Arrival Times.

changes which may affect the properties of the test fibers. Referring back to the basic strain measurement equation (3) in Chapter III, it is obvious that knowledge of not only the time parameters t and Δt, but also of the group index parameters, n and Δn, is important. The accuracy with which t and Δt can be measured depends solely on the characteristics of the OTDR unit. The precise determination of n relates back to the accuracy with which group index can currently be measured. Fiber manufacturers can specify this parameter to up to five decimal places. Even then, it is still required to take temperature changes into consideration. Reference [16] briefly discussed these effects for one way pulse delay measurements. The changes in time delay, τ, with respect to temperature, T, were given as:

$$\frac{\partial \tau}{\partial T} = \frac{1}{c}\left(\frac{\partial n}{\partial T}\, l_f + n\, \frac{\partial l_f}{\partial T}\right) , \qquad (17)$$

Where: $$\frac{\partial l_f}{\partial T} = \alpha l_f . \qquad (18)$$

α is the effective coefficient of thermal expansion of the coated fiber, and is in the order of $7 \times 10^{-7}/°C$. However, the changes of n with respect to T are in the order of $2 \times 10^{-5}/°C$ (B_2O_3-SiO_2), and predominate over the fiber length changes. This implies that for temperature changes of +/- 50 °C about room temperature it is possible to see changes in n of up to 0.001.

6.3 Strength Contribution of Fiber Coatings

In the experimental section it was mentioned that the discrepancy between the measured and predicted strain values may have been the result of neglecting the strength contributions of the fiber coatings. For fibers with high modulus, large diameter coatings it becomes necessary to take their strength contributions into account. For fibers with r layers of coating material, each having a Young's modulus, E_i, and cross sectional area, A_i, equation (15) becomes:

$$\varepsilon_f = \left(\frac{F}{\sum_{i=0}^{r} A_i E_i}\right) \quad . \qquad (19)$$

For fibers with coatings out to 500 micrometers (as was the case with the 100/140 μm fiber used in the experiments) and Young's moduli on the order of 500 N/mm^2 an overall strength increase of up to 8% can be expected.

Chapter VII

APPLICATIONS

7.1 Structural Stress Analysis

The applications of the local strain sensor are currently limited by the picosecond resolution of available OTDR systems. This implies that strain resolution is directly proportional to the length of fiber being used and the time allowed to perform SNR improvement (signal averaging). These two conditions make the sensor suitable for large structures experiencing slowly varying stresses. These structures include fiber optic cables during installation and/or operation across temperature, pipelines exposed to varying climatic conditions, and space structures undergoing low frequency vibrations, for example. Embedding of the local strain sensor in two or three dimensional arrays in structures such as graphite epoxy laminates should prove advantageous over conventional resistance strain gauges. Wire routing of these gauges is complex and, at instances, can affect the strength of the structures. A high-order fiber optic switching scheme would be required to allow access to the individual fiber arms of the array (see Figure 7.1).

7.2 Elastomeric Fiber Optic Splices

An indirect application of the air gap splice results

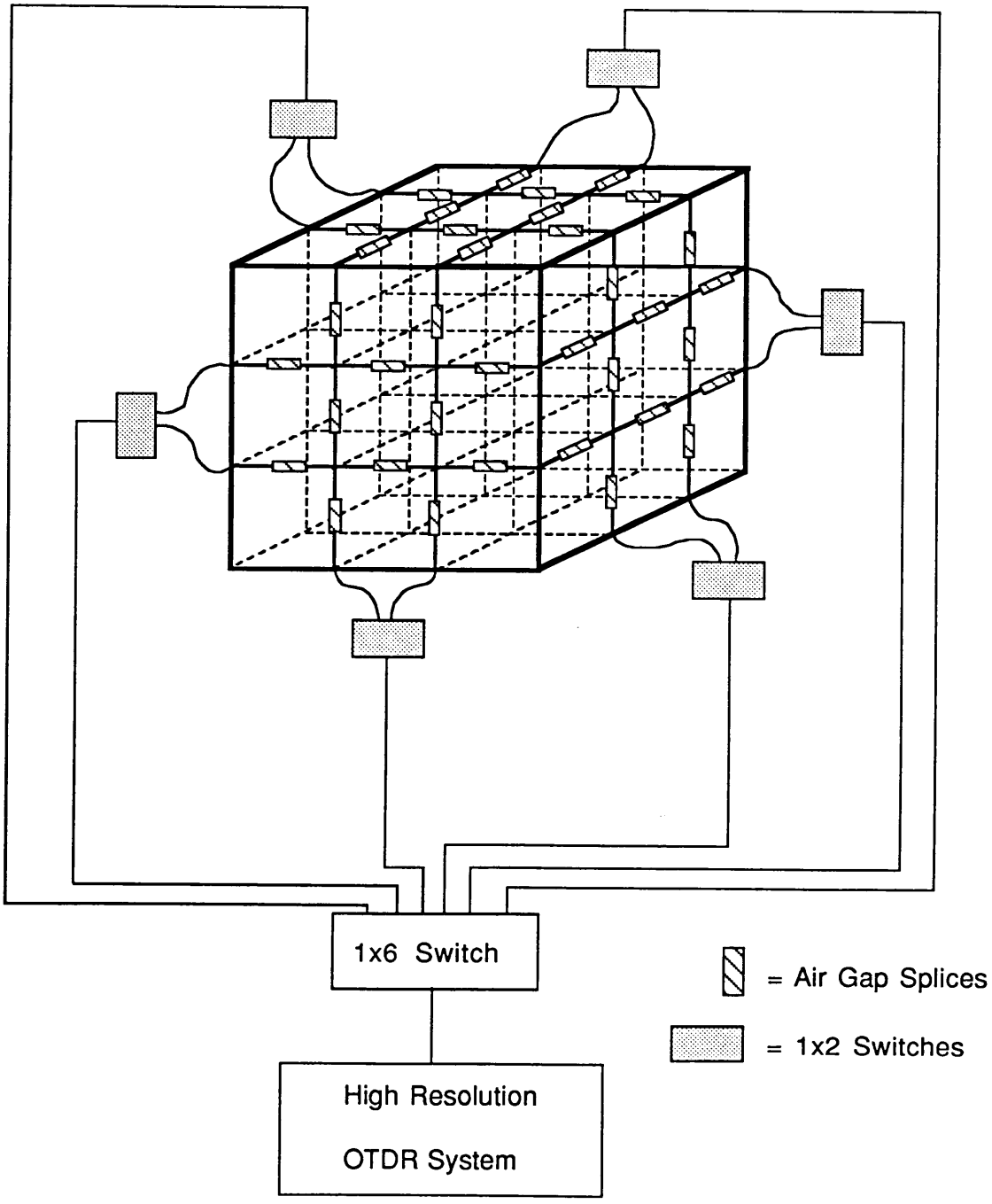

FIGURE 7.1 Application of the Local Strain Sensor in a Three Dimensional Structure with a High-Order Switching Scheme.

when considering the purpose of the alignment sleeve. This sleeve originally consisted of a section of fiber coating that had been pulled off a 100/140/500 micron fiber. It was difficult to insert the fiber ends into the 140 micron orifice, and usually resulted in coating particles being pushed into the alignment cavity. However, if a conically shaped "guidance tunnel" could be formed at each end of the alignment cavity, the before mentioned coating particles could be avoided inside this cavity. This resulted in the development of a low cost, easy to manufacture, fiber optic elastomeric splice.

The basic principle behind the splice manufacturing process consists of using a cylindrical rod such as the fiber itself as the alignment cavity molding object. A drawn-down glass capillary, as shown in Figure 7.2, would be inserted at both ends of a regular capillary filled with a curable elastomeric material. After the material has cured, the capillary "funnels" and the cylindrical rod (fiber) are pulled out leaving behind the desired guidance tunnel and alignment cavity (see Figure 7.3).

Initial splice evaluation testing indicates that the proposed splice, which measures half the size of the smallest elastomeric splice on the market, yields acceptable performance (< 0.2 dB loss) for multimode fibers. Further

elastomeric material evaluation is required, however.

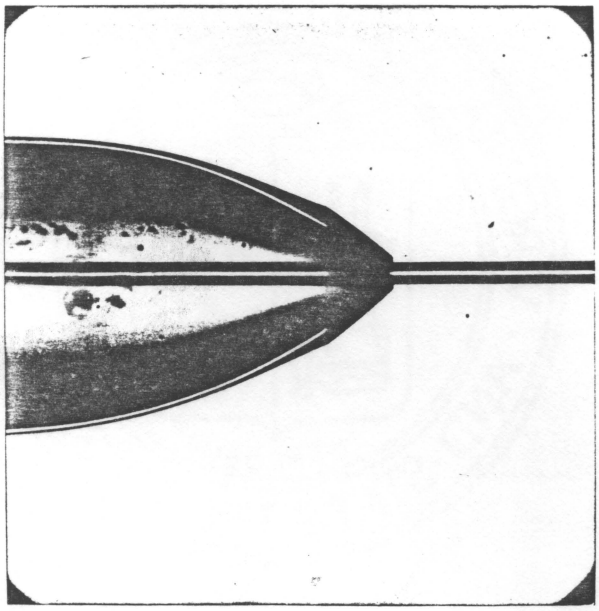

FIGURE 7.2 Drawn-Down Glass Capillary with Protruding Fiber, to be Inserted in the Elastomeric Splice Capsule.

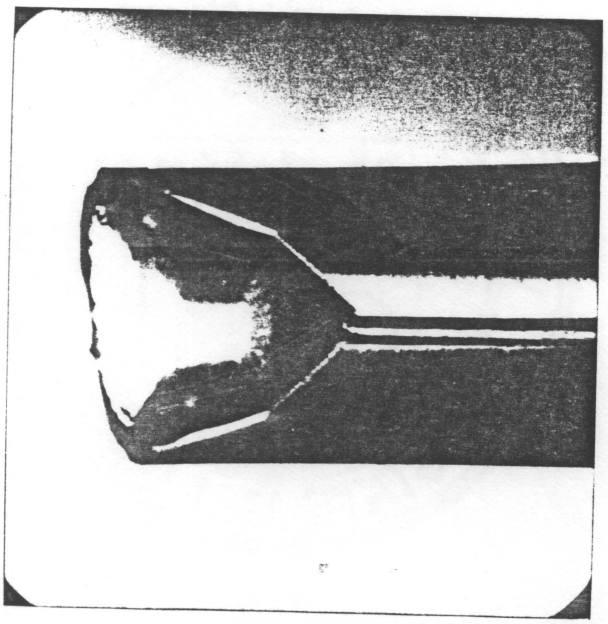

FIGURE 7.3 Elastomeric Splice after Removal of Drawn-Down Capillaries and Fiber.

Chapter VIII

CONCLUSIONS

It was shown herein that Optical Time Domain Reflectometry techniques can be applied for the determination of fiber strain on relatively short sections of fiber. With the given system, which utilizes a 400 ps FWHM pulse and a 50 ps jitter pulse delay generator, the spatial resolution was in the order of 4 cm. The strain resolution per meter of fiber was approximately 0.5 %, given that 100 averages were used per measurement. Ultimate strain resolution per meter with available narrow pulse, low jitter OTDR systems should fall in the 0.01 % range.

Furthermore, it was demonstrated that fiber segmentation allows the determination of local fiber strain. Experimental results indicate that, after determining some specific fiber properties, it is possible to match the predicted local strain values. Several variables need to be taken into consideration, however, to accurately determine local fiber strains. Of particular importance is the strength contribution of the fiber coatings, which may cause up to 8% inaccuracies.

Finally, it is worth mentioning the development with

respect to the elastomeric fiber optic splice. Considering that size of the segmentation device is crucial to the feasibility of the local strain sensor, it is obvious that currently available splices are too large for the proposed method. The developed elastomeric splice, measuring 1.2 by 19 mm may very well be suitable for these purposes. Losses for multimode fibers are in the order of 0.2 dB.

REFERENCES

[1] Optical Fiber Characterization, Vol.1, NBS Special Publication 637, July 1982, pp. 1-46.

[2] B. L. Danielson, "Optical Time Domain Reflectometer Specifications and Performance Testing", Applied Optics Aug. 1985, Vol. 24, No. 15, pp. 2313-2321.

[3] R. M. Clarke, "Optical Time Domain Reflectometer Specs Tell a Confusing Story," Electronics Test, Feb. 1987, pp. 37-39

[4] R. E. DuPuy, "The Present and Future OTDR," Aug., 1985, Proceedings of the 29th Annual SPIE International Symposium, pp. 83-87

[5] C. G. Bethea et al, "Photon Counting Optical Time Domain Reflectometer using a Planar InGaAsP Avalanche Detector", Electronics Letters, March 1986, Vol. 22, No. 6, pp. 302-303.

[6] B. F. Levine, C. G. Bethea, "Room Temperature 1.3 um Optical Time Domain Reflectometer using a Photon Counting InGaAs/InP Avalanche Detector", Applied Physics Letters, Feb. 1985, Vol. 46, No.4, pp. 333-335.

[7] B. F. Levine, C. G. Bethea, J. C. Campbell, "1.52 um Room Temperature Photon Counting Optical Time Domain Reflectometer", Electronics Letters, Feb. 1985, Vol. 21, No. 5, pp. 194-196.

[8] Opto-Electronics Inc., "Millimeter Resolution OTDR System", March 1987 Sales Brochure.

[9] K. H. Hafemeister, T. C. Clarke, "Automated Differential Fiber Strain Measurement System for Single and Multimode Fiber", 1984 NBS Symposium of Optical Fiber Measurements, pp. 81-84.

[10] C. K. Asawa, S. K. Yao, "Microbending of Optical Fibers for Remote Force Measurements", United States Patent # 4,421,979, Dec. 20, 1983.

[11] M. L. Henning, R. L. Langston, "Optical Sensing Systems", United States Patent # 4,653,916, March 31, 1987.

[12] G. W. Scherer, "Stress Induced Index Profile Distortion in Optical Waveguides," Applied Optics, June 1980, Vol. 19, No. 12, pp. 2000-2006.

[13] D. L. Philen, P. D. Patel, "Measurements of Strain in Optical Fibre Cables using a Commercial Distance Meter," 1982 ECOC Procedures, pp. 256-259.

[14] C. D. Butter, G. B. Hocker, "Fiber Optics Strain Gauge," Applied Optics, Sept. 1978, Vol. 17, No.18, pp. 2867-2869.

[15] B. D. Zimmermann, K. A. Murphy, R. O. Claus, "Local Strain Measurements using Optical Fiber Splices and Time Domain Reflectometry," 1987 Review of Progress in Quantitative NDE, in printing.

[16] AMP Inc., "Designer's Guide to Fiber Optics," 1982, pp. 52-59.

[17] D. Marcuse, "Reflection Losses from Imperfectly Broken Fiber Ends," Applied Optics, Dec. 1975, Vol. 14, No. 12, pp. 3016-3020.

[18] L. G. Cohen, J. W. Flemming, "Effect of Temperature on Transmission in Lightguides," Bell System Technical Journal, April 1979, Vol. 58, No. 4, p. 945.

[19] C. H. Lee, "Picosecond Optoelectronic Devices", 1984, Chapter 4: Picosecond Photoconductors: Physical Properties and Applications, pp. 73-117.

The vita has been removed from the scanned document